Never Landing Drone

Master of Science Thesis

By

C.P.L. de Jong

in partial fulfilment of the requirements for the degree of

Master of Science
in Control and Operations

at the Delft University of Technology,
to be defended publicly on Thursday January 7, 2020 at 10:00 AM.

Student number:	4384385	
Thesis committee:	B.D.W. Remes,	TU Delft
	G.C.G.E. Guido de Croon,	TU Delft
	C. de Wagter,	TU Delft
	M.B. Zaayer,	TU Delft

Never Landing Drone

Journal Title
XX(X):2–16

DOI: 10.1177/ToBeAssigned
www.sagepub.com/

SAGE

C.P.L. de Jong and B.D.W. Remes

Abstract

Increasing endurance is a major challenge for battery-powered aerial vehicles. A method is presented which makes use of an updraft around obstacles to decrease the power consumption of a fixed-wing, unmanned aerial vehicle. Simulatory results have shown the conditions that the flight controller can fly in. The effect of a change in wind velocity, wind direction and updraft has been analysed. The simulations showed that an increase in either updraft or absolute wind direction decrease the throttle consumption. A change in wind velocity results in a shift of the flight controller's boundaries. The simulations achieved sustained flight at 0 per cent throttle. The practical, autonomous tests reduced the average throttle down to 4.5 per cent in front of the boat. The unfavourable wind conditions and inaccuracies explain this minor throttle requirement during the final experiment.

Keywords

soaring, updraft, orographic lift, fixed-wing, flight control, simulation, practical tests

Introduction

While the usage of autonomously flying vehicles is increasing, and people are getting more confident with new technologies, a shift towards sustainable energy is also noticeable. It will not be possible in the future to design everything on fossil fuels, and either regulations or restrictions are appearing, which hinder the development of wasteful energies or support the use of sustainable products. Even though it is possible nowadays to fly up to 15000 km on a commercial aircraft, this can not be achieved using electrical energy. The main reason for this is the lower energy density of batteries compared to fossil fuels.

The same reasoning applies to the usage of Unmanned Aerial Vehicles (UAV). Current projects mainly lack the endurance and range to become successful. While drones can increase efficiency in numerous processes, they still lack battery power to replace the prevailing technology. Although battery efficiency is continuously improving, engineers are required to come up with alternative technologies to overcome this barrier. One of these is soaring: a technique which extracts energy from the wind. Previous research has shown that only wind energy can deliver the entire world with electricity. Miller et al.[1] provided an estimate of 18 to 68 TW that can be extracted using onshore energy. Jacobson and Archer[2] showed that even 80 TW would be possible in case one included offshore energy extraction. Physical limits and losses reduce these numbers to a lower estimate. Nevertheless, the demand for wind energy is increasing, and new technologies are able to increase the efficiency significantly.

Soaring has already been discovered in 1883. Inspired by Albatrosses, Lord Rayleigh discovered the first soaring technique. In his research, he proposed the dynamic soaring manoeuvre[3]. Subsequently, it was found that many other birds were

Email: chris@dejong.lu

able to fly nearly indefinitely without flapping their wings. Examples include Albatrosses[4,5,6], Andean Condors[7], Frigatebirds[8] and many more. Allen[9] has shown in his simulations that soaring can increase the endurance of UAVs in the summer from 2 to 14 hours. This finding could increase the use-cases for drones significantly.

Soaring has since been split up into two categories, static soaring and dynamic soaring. Static soaring makes use of a constant upward wind to gain energy. The wind can either come from thermals or any obstacle generating a vertical component of wind (orographic lift). Dynamic soaring makes use of a wind gradient to increase the relative air velocity between cycles.

While much work has been performed on dynamic soaring[4,6,10,11,12], less research is available on static soaring. The main contributors in this field are either UAVs using thermals to glide indefinitely[9,13,14] or research on static soaring techniques in urban environments[15,16,17,18]. The main reason for this is believed to come from the fact that static soaring is in general only useful in case the drone is stationary. Several limitations are present during static soaring. Gliders either need to move from one updraft to the next one, or they have to hover above the same spot.

This paper aims to analyse whether autonomous flight without usage of throttle is possible in the wind field generated by a moving obstacle. Using a moving obstacle allows following a predefined flight path. In case an excess of energy can be extracted from the wind field, not only will 0 per cent throttle be possible, but the remaining energy could also be used for other purposes. The critical wind conditions under which indefinite soaring is possible and the limitations of the flight controller will be investigated. Manual flights at stronger winds, conducted before the start of this research, have shown already that flying without throttle is indeed possible. This paper contributes to the development of a novel control method for autonomous and throttle-less soaring in front of a moving obstacle. By performing both simulations and practical tests, this paper aims to investigate the wind conditions under which the flight controller is able to soar indefinitely.

First, both the simulatory and experimental setup that is available for testing is introduced. After that, the flight controller is presented and then, the results and discussion of the simulations is given. The last section then gives the experimental results and their interpretation.

Method

This section of the report provides an overview of the research environment itself. The first subsection summarises the theory behind orographic lift in general and explains how it can be achieved using simple formulas. Then, both the simulation setup, as well as the experimental setup, are explained. Subsequently, the actual flight controller is illustrated.

Theory

Literature from Lee, Longo and Kerrigan[19], as well as from Patel[20], shows that the effect of the updraft can be modelled into the differential equations of motion by adding the relative motion between the air and the ground. Assuming that the UAV rotational rates are small and that control surface deflections do not affect forces, the relative motion of the UAV with respect to the ground is given by Equation 1.

$$\dot{z} = V_{TAS} \cdot sin(\gamma) + w_z \tag{1}$$

Here, the geographical height is given by z. V_{TAS} is the true airspeed, γ is the flight path angle, and the wind velocity in the z-direction is given by w_z.

In order for the aircraft to fly indefinitely, the vertical wind speed has to be at least as high as the minimum rate of climb. This condition is stated by Equation 2 .

$$\dot{z} \geq 0 \Leftrightarrow V_{TAS} \cdot sin(\gamma) \geq -w_z \tag{2}$$

As seen in the equation, the rate of climb is a function of both the true airspeed and the flight path angle. The true airspeed for a given position is mainly dependent on the horizontal wind speed at that location. The flight path angle, on the other hand, is dependent on the angle of the wind vector. Depending on this angle, the UAV changes its angle

of attack in order to keep forces in equilibrium. The flight path angle at a given location can then be calculated using the knowledge of both aircraft angle of attack and incoming wind angle. A general sketch of all the related variables is given in Figure 1.

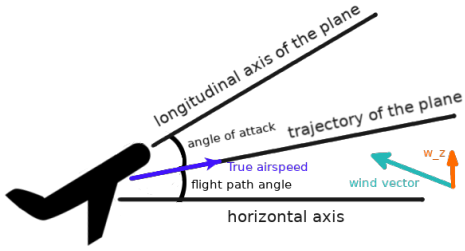

Figure 1. Sketch of general flight variables.

Simulation Setup

The general SIM environment of the paparazzi UAV software will be used as the primary simulation environment*. This is an essential fixed-wing simulator without inertial measurement unit simulation or any sensor models.

The paparazzi environment comes with a ground Global Positioning System (GPS) module sending the ground station position to the UAV. The movement of the boat is simulated by changing the lateral and longitudinal position of the ground gps module in the simulation. This position can be increased in both directions by a predefined value at each timestep.

The last component that needs to be simulated in the testing environment is the wind flow generated around the boat. Paparazzi comes with the built-in gaia module, which makes it possible to set speed, direction and updraft of the wind for the whole simulatory environment. In practice, however, both the updraft and the horizontal wind speed are far from being uniform around a hill shaped object[21]. The flow around a boat is even more complex. This work thus assumes a constant wind speed and wind direction for the simulatory analysis.

To test the flight controller, a couple of experiments are performed that investigate the power consumption over a range of different wind regimes. The parameters are given by a change in wind speed, wind direction and updraft.

Experimental Setup

To test the algorithm and analyse throttle performance of the flight controller in real flight, it is decided to use the fixed-wing model of Parrot, namely the Disco. The Parrot Disco is stable enough for flying inside these heavy wind conditions. The on-board pitot tube of the Parrot Disco also makes it possible to use airspeed related control loops instead of relying on GPS ground path tracking. A couple of modifications have been made to improve the overall performance. First, the general Parrot autopilot has been overwritten with the paparazzi UAV software to enhance the autopilot capabilities. Next, to obtain a better GPS accuracy, a u-blox M8P GPS module has been added. This makes it possible to correct for satellite propagation errors using Real Time Kinematic (RTK) positioning, and as such, provide up to centimetre-level accuracy.

For the research, testing of flight-related controllers will be performed in two different testing environments. First an emergency towing vessel has been made available by the dutch coast guard. Several manual flights in front of the boat have shown that its size and speed are sufficient to achieve throttle-less and autonomous soaring. The maximum speed of the boat is equal to 8.2 m/s, and with its width of 65 meters and height of 8 meters, it is able to generate enough updraft.

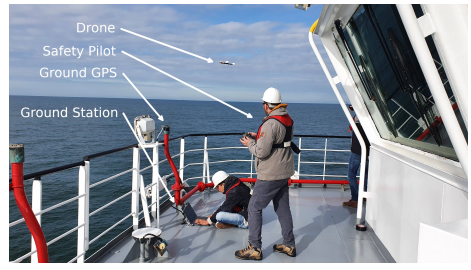

Figure 2. A general impression of the main test setup.

The ground segment consists of a laptop running the paparazzi UAV software. It is connected to

*http://paparazziuav.org/

the drone using Wi-Fi. An M8P GPS module is used to send satellite propagation errors and the current position of the boat to the drone. A general impression of the main experimental setup can be seen in Figure 2.

The second testing environment generates the updraft using dunes. In case wind direction and speed allow it, it is possible to soar indefinitely here as well. The test setup here will be equivalent to the main setup as described above. Instead of using the emergency towing vessel to generate the updraft, it is generated using the dune. This alternative flight setup is depicted in Figure 3.

Figure 3. Representation of alternative test setup experimenting with dunes.

The main difference between both environments is that the drone is stationary in case it is flying at the dune. Heading related information can thus not be obtained from GPS positions, and the usage of a magnetometer is required. Furthermore, achieving stationary flight at the dunes is easier compared to achieving hovering flight in front of the boat. This comes from the fact that the ground speed is constant for dune flying. The ground speed prediction of the boat, however, is dependent on the GPS positions received by the ground station. These positions come with errors and hence the desired speed is fluctuating more. Furthermore, for dune flying, the area in which the updraft is available is bigger and thus the changes in updraft along the width are smaller. For the boat, this area is limited by the width of the boat itself. This gives the flight controller a higher margin for error in the former case. Last, dune flying is more tolerant to failures. A failure here simply results in a ground crash. A failure in front of the boat will result in a crash into the water or the boat will collide against the drone.

Flight Controller

The central part of the current research is focused on changing the outer loop of the paparazzi UAV flight controller. This loop is responsible for the navigational routine. Based on waypoints, this loop sets the desired flight attitude and speed. Both of these desired parameters are then sent to the inner loop to obtain the required elevon deflections. The algorithm is based on a waypoint located at a specified position to the ground GPS module. Based on this waypoint, the positional errors to the desired location are calculated. A top and side view of both of these errors to the UAV is given in Figure 4.

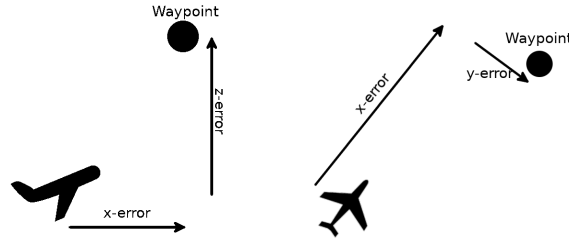

(a) Side view. **(b)** Top view.

Figure 4. Reference position for the computations of positional errors towards the desired waypoint.

Positioning of the waypoints is currently done by the safety pilot. Once a spot with favourable wind conditions is found, the safety pilot switches to autonomous mode and the flight controller immediately sets its waypoint to the current location. The current positional strategy is thus enforced by the safety pilot.

The GPS coordinates of the ground station are sent with a period of 1 Hz. Each time that new GPS coordinates are available, the UAV resets the waypoint with respect to the current ground station position. Based on the new waypoint location, the UAV calculates the positional errors and translates them to desired pitch and roll angles, as well as to the desired airspeed.

The energy control loop of the paparazzi UAV autopilot project is used for the autopilot. The main reason for this is the fact that autonomous orographic soaring consists in simple terms in an exchange between potential and kinetic energy. Whenever the UAV is located too far upstream, it has to trade some of its kinetic energy with potential energy to reach the feasible soaring region. Otherwise, in case the UAV is located too far downstream, potential energy has to be exchanged to kinetic energy.

This exchange in energy must be regulated by an additional module. Three different loops have been added to the algorithm, namely, a throttle, a pitch and a roll loop. The throttle loop is responsible for adjusting the motor speed based on the requirements needed to soar. The pitch and roll loop are in charge of the respective angles. The following paragraphs illustrate the process of each of the loops.

First, the throttle loop adjusts the motor speed of the UAV. With an ideally tuned controller, this loop should decide to use no energy at all and leave the power consumption of the motor at 0%. However, due to safety reasons, it was decided to allow minor throttle components in case the UAV is located too close to the boat, or if the UAV is not able to reach its climb setpoint using exclusively the pitch controller.

A block diagram of the throttle controller is given in Figure 5. As can be seen, the controller takes as input the positional x-axis error. Based on this distance, the throttle controller calculates the *air_inc* variable. This is the difference in airspeed that is required by the PID loop. The new desired airspeed is then averaged to reduce the ON-OFF behaviour of the engine in case the x-error is jumping between a positive and a negative value. These jumps are mainly due to both ground GPS and on-board GPS inaccuracies. Averaging also ensures that the throttle loop lags behind the pitch loop and as such only commands an increase in throttle in case it is really required. The airspeed setpoint is then bounded between the minimum and maximum values and send to the inner loop of the flight controller. The inner loop of the airspeed controller is tuned in such a way, that only a proportional and a small integral term remain. This will make sure that the proportional term starts the motor if the UAV is located too far behind the waypoint. This also ensures that the UAV will not crash into the boat during sudden wind gusts propelling it backwards. The integral term is responsible for removing UAV oscillations around the waypoint. In case the wind is too strong, the integral term of the flight controller guarantees that a minimum amount of throttle is constantly used to overcome drag forces if required.

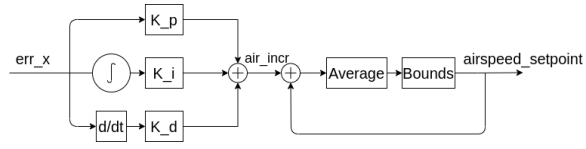

Figure 5. Block diagram of the throttle controller.

Second, the pitch loop is responsible for adjusting the pitch setpoint of the UAV. During autonomous soaring, a pitch up movement is used to increase the horizontal drag of the UAV and move backwards. The same reasoning applies to a pitch down movement, decreasing drag and thus moving forward. An exchange from potential to kinetic energy also explains this decrease and increase of ground speed due to a change in drag. Pitching upwards results in gaining height and losing airspeed while pitching downwards results in losing height and gaining airspeed. Next to this, the pitch loop is also responsible for reaching a specific altitude. The internal paparazzi energy loop incorporates already all the required algorithms for tuning of climb and airspeed related gains. On top of this, a term has been added to the pitch loop, which increases the pitch angle depending on the relative position of the UAV with respect to its soaring waypoint.

A basic block diagram of the pitch controller is shown in Figure 6. Here the x-axis error is also used as input. The pitch increment based on the

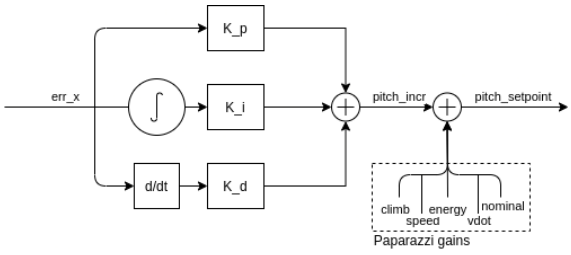

Figure 6. Block diagram of the pitch controller.

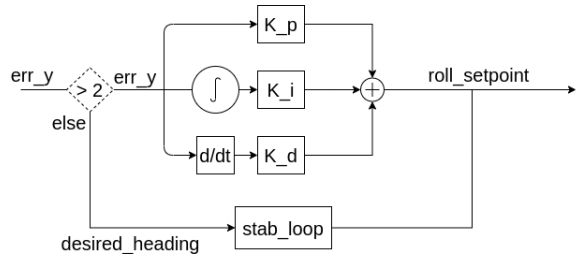

Figure 7. Block diagram of the roll controller.

soaring distance consists of a simple PID controller. After that, the respective gains of the energy loop are added. 'Climb' is the pitch setpoint based on the altitude error, 'speed' based on the speed error, 'energy' based on the kinetic energy that we want to turn into potential energy, 'vdot' based on a derivative term of the speed error and finally a nominal value which is calculated using an integral error.

Even though both, the pitch and the throttle loop are used to nullify the x-axis error, they are both used for a different purpose. The pitch loop is responsible for trading excess potential energy into kinetic energy. The throttle loop, on the other hand, is only needed in case the pitch loop is not able to set both climb and speed requirements simultaneously. These limitations will be explained in the upcoming sections.

Last, the roll loop consists of a simple PID controller. Using the y-axis positional error, this controller is only activated in case the UAV is more than 2 meters away from its target. In case we are already flying on the waypoint, the heading is simply set equal to the heading based on the GPS positions received by the ground station. In this case, the internal paparazzi roll loop can cope with the positional requirement. However, as soon as the y-positional errors become too large, the roll controller is used to put the UAV back towards its desired waypoint. After that, heading based flight can be resumed. The final roll loop is represented in Figure 7.

Simulation

In this section, first the results of the different simulations are given. Then, a follow-up discussion will interpret and explain the results.

Simulatory results

The first performed experiments monitor the power consumption of the UAV for a changing wind speed and updraft. For this, the above-mentionned flight controller has been subjected to a range of different wind speeds and updrafts. The position in front of the boat had to be kept for around 60 seconds at each wind condition. The speed of the ship is simulated with an average speed of around 4 m/s.

Simulations have shown that 2 limiting cases exist for the flight controller. The upper limiting case at maximum throttle, and the lower limiting case at minimum throttle.

The lower limiting case is illustrated in Figure 8. As can be seen, here the throttle is reaching the 0% condition. Thus this limitation is more prevalent during autonomous soaring. A decrease in either the relative horizontal wind speed or an increase in updraft will result in a required throttle below 0 per cent. This is not feasible and hence this condition results in the flight controller losing track of the waypoint and flying away from the boat. Additionaly, it can be noticed, that the altitude error is decreasing (and hence the altitude increasing) significantly during this manoeuvre.

The upper limiting case is presented in Figure 9. Increasing either the horizontal wind speed or decreasing the updraft will result in the UAV colliding against the boat. Before the collision, a

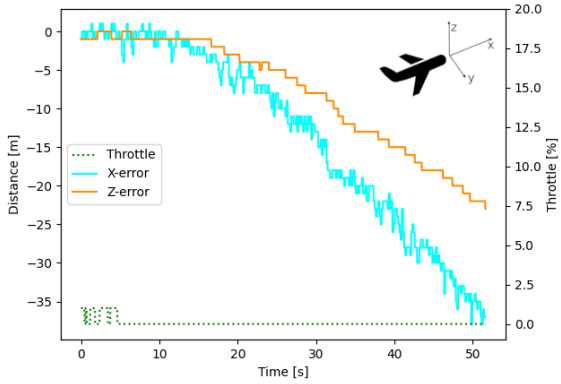

Figure 8. Lower limiting case at minimum throttle.

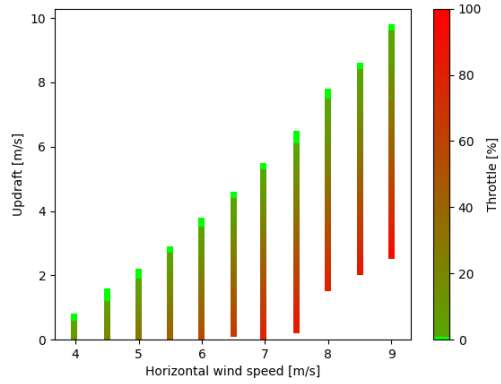

Figure 10. Feasible flying region for a range of alternative wind conditions.

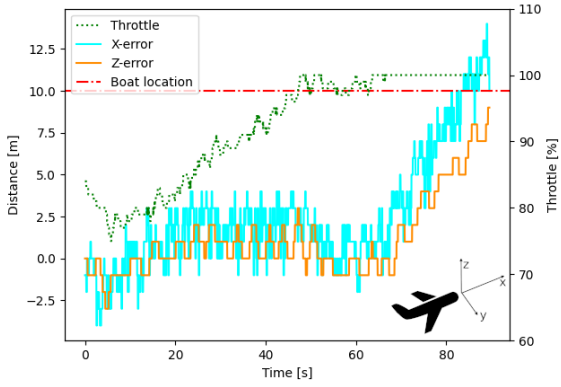

Figure 9. Upper limiting case at maximum throttle.

decrease in altitude can be observed. While the figure illustrates a case where 100 per cent of throttle was achieved, it should be noted that this lower case can also exist at lower throttle. This phenomen happens whenever the throttle controller can not compensate for the pitch errors created at the given wind conditions anymore.

Using the knowledge of the above-mentioned boundaries, it is possible to assign a feasible flying regime to the current flight controller under atlernative wind conditions. The feasible flying region is given by all the wind conditions in which the flight controller is able to hover within a 5-meter accuracy of its waypoint with full access to the throttle. The final wind regime results are depicted in Figure 10.

The first thing that can be observed in Figure 10 is the fact that the UAV needs a minimum horizontal wind of 4 m/s for autonomous hovering. Furthermore, it is noticeable, that up to a wind speed of 7 m/s, an increase in wind speed increases the lower limit of the feasibility region. Consequently, increasing the wind speed beyond this point, will result in the upper limit exceeding 0 m/s updraft and increasing even more with an increase in horizontal wind speed. The same applies to the lower limit. Increasing the horizontal wind speed will allow for a larger lower limiting case. Moreover, the Figure shows the minimal size of the region where sustained flight at 0 per cent throttle is possible. While the UAV is able to hover at a large wind regime, only a smaller subset of this wind regime allows autonomous soaring without motor. Furthermore, the required updraft increases significantly with an increase in horizontal wind speed. A wind speed of 4 m/s requires an updraft of 1 m/s for autonomous and throttle-less soaring. Doubling the horizontal wind speed to 8 m/s, however, requires already an updraft of 7.5 m/s.

From the above discussion, it is decided to use a wind velocity of 4.5 m/s with an updraft of 1.1 m/s while operating the ship at a cruise speed of 4 m/s for further simulations. This comes from the fact that a lower horizontal wind velocity allows for a larger 0 per cent throttle region. Additionally, it is assumed that the 4 m/s wind regime is too small for further testing. Based on these properties, a long flight simulation of 90 minutes has been executed to validate whether the flight controller is able to keep its position and throttle. The results are presented in Figure 11.

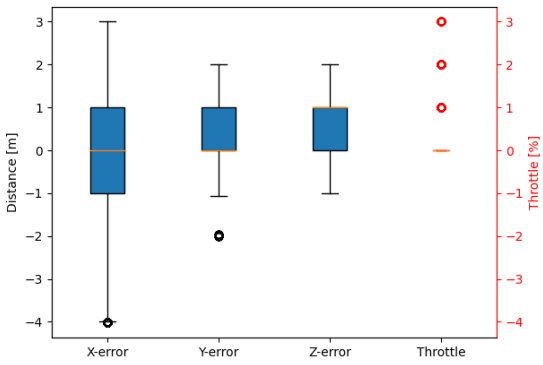

Figure 11. Boxplot distribution of main parameters during a 90 minutes flight simulation.

The graph shows that throughout the entire flight, the throttle is kept at nearly 0%. The four quartiles of the throttle each correspond to 0, meaning that nearly all datapoints lie at 0%. Only a couple of outliers are detected from one to three per cent of throttle. Next to that, it is shown that the roll controller is able to keep the lateral distance in the y-direction. The x-positional error, however, is fluctuating more. The inter-quartile range shows that 50% of the data points lie within a 1-meter accuracy of the desired waypoint. Thus, half of the flight, the UAV can hover within 1 meter in longitudinal distance. The minimum and the maximum error lie at -4 and 3 meter, showing that a minor bias is detected for flight in front of the waypoint. The same applies to the z-distance. Here 50% of the data points are within 1 meter below the waypoint. The remaining 50% span the range from -1 to 2 meter. In general, Figure 11 shows that the UAV is able to hover accurately at the waypoint location. A small bias is detected for flying in front and below the waypoint.

The next simulation looks into the effect of wind direction on the fly conditions. The wind direction is defined as the angle spanned by the boat velocity and the negative horizontal wind velocity. The simulation parameters are a horizontal wind velocity of 4.5 m/s, an updraft of 1 m/s and a boat velocity of 4 m/s. The initial wind direction is given by 0°. It is then incremented gradually in steps of 1°. For each iteration, the UAV tries to hover at the waypoint for 60 seconds. The results of the average power consumption for each wind direction are illustrated in Figure 12.

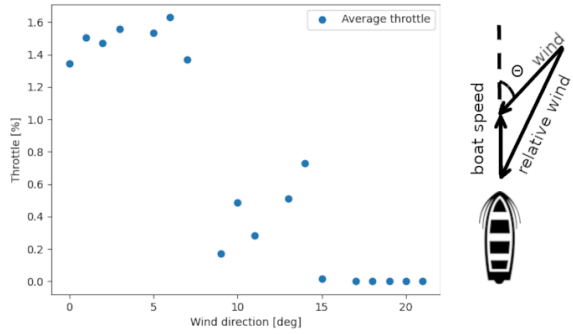

Figure 12. Power consumption of the flight controller for a range of different wind directions.

As can be observed, with the afore defined wind conditions, the flight controller can keep its position up to an absolute wind direction of 21°. Exceeding this wind direction, the relative velocity of the wind was too slow, and the UAV started losing track of its waypoint. As a result it is flying away from the boat with an increase in altitude. Figure 12 demonstrates that with an increasing absolute wind direction, the flight controller needs less throttle. The autonomous flight without usage of throttle is achieved at an absolute wind direction of 20°. At a straight wind of 0°, however, around 1.4% of throttle must be used.

The explanation for this behaviour is given in the subsequent discussion.

Simulatory discussion

As presented in the previous subsection, the simulatory results consist of a set of different flight conditions and depict a couple of interesting phenomenons.

First, it was found that two limiting cases exist for the flight controller. The lower case resulted in the UAV flying out of its flying region and away from the boat. This case could only be attained in case minimum throttle was reached. Increasing either the updraft or decreasing the horizontal wind speed ensured that the UAV lost track of its waypoint. The reason for this behaviour comes from the stall speed requirement incorporated in the paparazzi energy loop. By decreasing the horizontal wind velocity, whilst following the ground speed of the boat, the desired airspeed reached values below the stall speed. The paparazzi energy loop then overwrites the desired value of the flight controller and sets the desired ground speed such that the UAV flies at minimum stall speed. A similar reasoning applies to an increase in updraft. As the UAV is flying at stall speed already, and hence at maximum lift coefficient, it is in a highly pitched up flight condition. A higher updraft then results in a gain of potential energy, which has to be converted to kinetic energy to satisfy the altitude requirement. This produces a gain in airspeed and by such a gain in ground speed. In both scenarios, the UAV flies away from the ship. This case was also accompanied by an increase in altitude. The fact that the UAV is flying away from the waypoint means we obtain a high x-axis error. To compensate for this error, the pitch controller pitches up. This in turn results in a gain of potential energy and by such an increase in height. The lower limiting case is thus due to an excess of either kinetic or potential energy. While the throttle can not be reduced any further to consume this overshoot in energy, an energy harvesting system could be implemented in the controller. This energy harvesting system would serve two advantages. First, flight at higher updrafts would be possible and the lower limiting case would be shifted upwards. Second, harvesting the excess energy makes it possible to charge the batteries in flight and by such further improve the endurance of the flight controller itself.

The same applies to the upper limiting case. Here the UAV either dives into the sea or crashes against the boat due to a decrease in updraft or an increase in horizontal wind speed. The reasoning behind these manoeuvres comes from the fact that the UAV is flying at maximum throttle already. A higher relative horizontal wind speed will result in an increase in drag. This leads to a lower ground speed. The natural reaction of the flight controller is to pitch down to transfer some potential energy towards kinetic energy. In case the horizontal wind speed is too strong, or the updraft is not strong enough, the UAV loses altitude and ground speed and hence crashes into either the boat or the sea. The same reasoning applies to a decrease in updraft at constant wind speed. The decrease in updraft results in a loss of potential energy. This loss in potential energy is counteracted by a pitch up movement, translating kinetic energy towards potential energy. As the throttle controller is saturated already and no additional energy can be gained, the UAV is not able to satisfy its ground speed requirement and crashes into the boat.

The analysis of the feasible flying region has shown that a minimum horizontal wind speed of 4 m/s is required for autonomous hovering. This is traced back to the fact that the stall speed of the Parrot Disco is given by 8 m/s and the boat was driving at 4 m/s. A minimum wind velocity of 4 m/s is thus needed to satisfy the stall speed requirement. Subsequently, it was shown that at wind speeds above 7.5 m/s, no feasible hovering conditions could be achieved without any updraft. This minimum required updraft is due to the need of available total energy to increase the airspeed beyond these horizontal wind speeds. The same applies to the remaining limiting case. While the maximum updraft at 4 m/s was given by 0.7 m/s, the maximum updraft at 7 m/s of horizontal wind is given by 5.5 m/s. By increasing the updraft, the UAV is able to harvest more kinetic energy from its available potential energy, and hence the feasible flying region

shifts upwards. The final result obtained from the wind regime simulation confirmed that the throttle-less flying region is only a very small subpart of the actual feasible flying region. This is linked to the fact that autonomous soaring is a trade-off between kinetic and potential energy. To use 0% of throttle, the available potential energy by the updraft needs to be sufficient to generate enough kinetic energy to overcome the wind conditions. Too much potential energy, however, will result in the lower limiting case. This means the UAV loses track of the waypoint due to either an excess of potential or kinetic energy. In the opposite case, decreasing the updraft and thus the potential energy at higher speeds, results in the UAV requiring an additional amount of total energy. This energy is obtained by an augmentation of throttle, which can not be achieved if the UAV has reached maximum throttle already.

In summary, the wind regime analysis has shown that autonomous soaring in front of a boat is nothing more than obtaining a certain amount of potential energy to hover at a given altitude, combined with obtaining enough kinetic energy to follow the ground speed of the boat. While the throttle controller is used to modify exclusively the kinetic energy, the pitch controller is used for trading kinetic energy with potential energy. Good positioning of the UAV in the wind field itself is then required so that neither an excess, nor a shortage of total energy is available. While an excess of total energy only results in the UAV flying away and losing track of the waypoint, a shortage of energy results in the UAV either crashing against the boat or into the sea. The latter is thus the critical case that should be avoided at any cost.

Next, the long flight simulation confirmed that the algorithm is able to keep a constant throttle value of 0% at optimum conditions. It is thus proven that throttle-less and autonomous soaring is possible in perfect conditions. The outliers presented at a range from 0% - 3% are explained by the p-gain which turned on the motor for a couple of seconds in case the pitch controller was not reacting fast enough. This means the current potential energy was misestimated, requiring an additional need of kinetic energy from the throttle controller. It has also been demonstrated that a small bias is detected for flying in front of the waypoint. This is associated with the fact that the proportional term for the throttle loop is used to aggressively move the UAV away from the boat. The bias obtained in the z-positional error for flying below the waypoint is also explained because of this. The flight controller has a preference for converting potential energy into kinetic energy, resulting in a minor bias for flying below and in front of the waypoint.

Finally, experiments on wind direction changes have demonstrated that the algorithm performs better in case the UAV is flying crosswinds. Flying crosswind results in the UAV experiencing a lower relative, longitudinal wind speed. This is due to the fact that the wind vector can be decomposed into a longitudinal component parallel to the flight path and a lateral component perpendicular to the flight path. The wind field analysis has shown beforehand that a lower longitudinal wind speed will reduce the drag. In order to maintain the same ground speed, the UAV thus requires less throttle. The same limitations as before apply as well. Autonomous hovering is only possible as long as the stall speed of the UAV is not reached. Increasing wind direction can thus be seen as decreasing longitudinal, horizontal wind speed. This discussion is only valid in case the same updraft can be obtained at a crosswind wind regime.

The final behaviour of the flight controller in different wind regimes is shown in Figure 13.

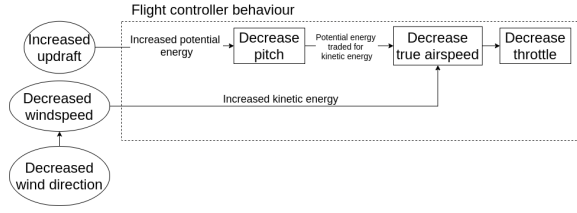

Figure 13. Functional block diagram of the flight controller process during a change in wind conditions.

From this behaviour, it can be seen that the boat holds a couple of options to improve the hovering capabilities. As such, accelerating the boat speed will increase both the relative horizontal wind and the updraft. This can lead to better hovering capabilities at different positions. Depending on the relative position of the UAV with the boat, this can decrease

throttle consumption. The updraft can be increased by changing the relative position of the UAV with respect to the boat, and in case too much horizontal wind speed is available, the boat can change its heading to decrease only the horizontal wind speed. Depending on the size and shape of the boat, similar updrafts should be generated.

Practical tests

This section first presents the results of the experimental tests and then draws conclusions based on the validity of the flight controller in the second subsection.

Experimental results

For the experimental results, the flights were mainly dependent on the weather conditions of the flight day. During the first flights, the main problem that persisted was a deviation of the UAV from its actual flight plan. This resulted in the UAV either crashing into the sea or the safety pilot taking over control. The problem was found to be a magnetometer error. Further investigation of the problem showed that the feasible soaring region was indeed too close to the ship. The metallic structure of the vessel interfered with the Earth magnetic field, and the UAV was not able to keep a constant heading anymore.

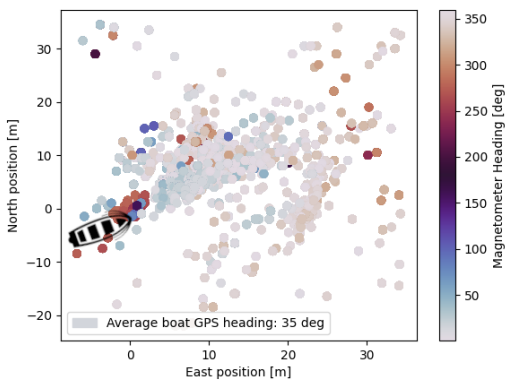

Figure 14. Magnetometer heading with respect to the relative position of the UAV with the boat.

Figure 14 shows the magnetometer heading to the relative position of the UAV with respect to the boat. For the depicted flight, the UAV was soaring constantly in front of the boat. The GPS coordinates from the boat show a path with an average heading of 35°. While this heading is also detected on datapoints further away from the ship, a significant difference can be seen between data points closer to the origin (ship). An average change in magnetometer heading of around 100° is noticeable

Instead of relying on the magnetometer measurements to obtain an accurate heading, GPS positions have to be integrated. This comes with the limitation that stationary flight in front of the boat will not be possible. Minor movement across the GPS position is required in order to obtain a correct heading. Figure 15 shows the GPS accuracy during the final flight. Even though a moving baseline RTK GPS has been used, the UAV was never able to achieve an RTK-fix using the satellite propagation errors received by the ground station. Merely one-third of the time a differential GPS fix has been attained with an average GPS accuracy of 1.1m.

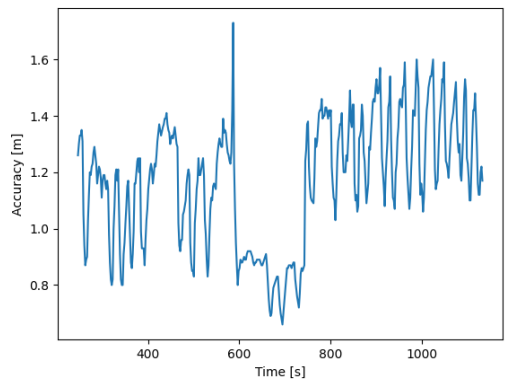

Figure 15. GPS accuracy during final flight.

After that, the average wind velocity during the testing day was only around 3 m/s. This resulted in the ship having to cruise at the nearly maximum speed of around 8 m/s in order to obtain feasible soaring conditions. The results of the final flight are

illustrated in Figure 16. During the experiment, the safety pilot intervened twice to reposition the drone to a new location with better soaring conditions. Furthermore, there were difficulties in tuning the roll controller, resulting in the roll angle to be set by the paparazzi energy loop instead of the roll controller.

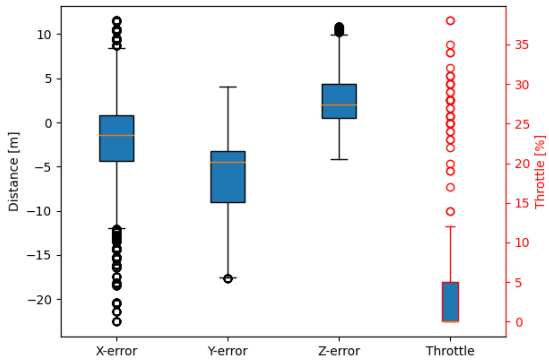

Figure 16. Boxplot distribution of main parameters during the final flight.

From Figure 16, one can deduce that the flight controller can reduce the throttle consumption significantly. During half of the flight, the controller could reduce the throttle to 0%. One quartile of the upper range corresponds to values below 5% and the remaining quartile in a range from 5% - 13%. Many outliers are, however, present up to a range of 37%. The average throttle consumption throughout the whole flight is given by 4.5 %. The y-error positional block shows a median value of -5 meters. Moreover, the lower quartile extends to a value of -17 meters, while the upper quartile only extends towards nearly 5 meters. Both of these observations confirm a tendency of the UAV to fly on the right side of its waypoint. The z-error positional block, demonstrates that the flight controller was able to keep its altitude quite accurately. 50% of the data points lie within 5 meters below the waypoint. Both the upper and lower quartile stretch to values of -5 and 10, respectively. Meaning that the UAV has a slight tendency to fly slightly below its actual waypoint. Finally, the x-error gives a more considerable margin of error. The controller can keep its longitudinal position 50% of the time inside a region of 4-meter accuracy. However, the whiskers of the box plot extend up to a 10-meter error. More outliers are detected with negative errors and both the lower quartile and the minimum extend further downwards compared to the upper quartile and the maximum. This shows a tendency of the flight controller to fly in front of the waypoint. The flight had to be terminated after 15 minutes of autonomous soaring at low throttle as the ship was leaving the testing area.

Experimental discussion

This section discusses the experimental test results and validates whether the flight controller is working as expected. First it was detected that the magnetometer could not be used to calculate the vehicle heading. The successful autonomous flight has shown that using a GPS integrated heading is sufficient for a ground speed of 8 m/s. It is recommended to test the GPS heading at lower ground speeds. This can result in the heading jumping more drastically. Additionaly, analysis of the GPS results also showed that instead of the desired centimetre accuracy, the RTK GPS module using a moving baseline was only able to achieve a differential GPS fix with an average accuracy of 1.1 m. For soaring and autonomous hovering, however, centimetre accuracy is desired as the wind conditions change drastically throughout the environment. Errors in the meter range can change the UAV from suddenly flying out of the feasible soaring region and by such increase throttle consumption or even make flying infeasible.

The throttle analysis showed that the experimental results are slightly worse compared to the simulations. While the simulatory flight was able to achieve throttle-less, autonomous flight, the experimental flight had multiple outliers in the 30% range. These, and as well the y-positional outliers, can be explained by the lower GPS accuracy. It is recommended to achieve an RTK fix in order to obtain the best results of the flight controller. Jumping from positions in front of the waypoint to positions behind the waypoint will result in heavy pitching behaviour, and the faulty positioning of the drone in

the wind field then leads to a loss of either potential or kinetic energy. Then, while the wind conditions are kept constant throughout the whole flight in the simulation, during the experimental flight a human operator had to set the position of the UAV in the wind field manually. This resulted in a higher throttle consumption at the beginning of the flight. A consecutive accurate positioning resulted in later stages of the flight in a decrease in throttle. Even though a lot of outliers are detected, the average throttle consumption was only 4.5% for the whole flight. This required a small amount of power from the battery, however, it should be noted that at an average throttle of 4.5% the propeller is barely spinning and thus providing no significant thrust. Further gain tuning should be sufficient to decrease these last percentages and allow throttle-less, autonomous flight at the given wind conditions.

Furthermore, a tendency to fly below and in front of the waypoint has been detected in the experimental flight. This is equivalent to the observations that have been made in the simulatory flight and has to do with the fact that the flight controller tends to translate more potential energy into kinetic energy. The gain in kinetic energy results in it flying further away from the boat for safety reasons and the loss in potential energy results in it flying slightly below its desired waypoint.

Finally, the lateral positional error is explained by the fact that successful tuning of the algorithm was not possible at the given flight conditions, and thus the paparazzi inner loop was responsible for lateral positioning. Instead of adjusting the heading to induce lateral movement, the inner controller tried to follow the heading of the boat itself. As such, it was constantly offset to the right.

Conclusion

A flight controller has been proposed which enables throttle-less and autonomous soaring in the wind field generated by a moving ship.

Based on the paparazzi UAV energy loop, the flight controller is able to achieve autonomous flight at 0 per cent throttle in the simulations. A practical test has confirmed that the throttle consumption can be decreased significantly in front of an emergency towing vessel. The flight controller was able to reduce the throttle consumption to an average of 4.5%. This minor required throttle is believed to come from unfavourable wind conditions during the day of testing. The positioning of the drone in the wind field itself and GPS propagation errors are also possible causes for this behaviour.

Using an equilibrium of both kinetic and potential energy, the flight controller enables autonomous hovering in a range of different wind conditions. Autonomous soaring without usage of throttle is only possible for a smaller subset of updrafts at a given wind speed. Lower updrafts proved to be feasible, but the throttle consumption increased with a decreasing updraft. Wind speeds beyond a specific range showed that a minimum updraft is required to stay aloft. Furthermore, two prominent limiting cases have been identified. The lower case resulted in the UAV flying away from its desired position due to stall speed requirements and an excess of energy. The excess of energy can in turn be harvested to avoid this flight behaviour and provide battery charging capabilities for example. The upper case resulted in the UAV crashing against the boat or into the sea due to a deficiency in either kinetic or potential energy.

Analysis of wind direction on the flight regime demonstrated that an increase in wind direction is favourable for autonomous soaring. Increasing the wind direction will result in a lower longitudinal wind speed. This slower wind speed will allow flight at lower kinetic energy and hence reduce throttle consumption. Increasing the wind direction beyond the point where the UAV starts stalling will result in a loss of the hovering capabilities.

As such, autonomous flight in front of a boat makes it possible to change the wind conditions according to the current needs. Increasing the boat speed will increase both the relative horizontal wind and the updraft. Depending on the relative position of the UAV with the boat, this can decrease throttle consumption. The updraft can be increased by changing the relative position of the boat with respect to the UAV, and in case too much horizontal wind speed is available, the boat can change its

heading in order to decrease only the horizontal wind speed.

Future work is suggested to improve GPS accuracy by improving the current moving baseline RTK technology. Research in additional geolocation systems such as fixed cameras on the boat or ultra-wideband radio technology can also increase the positioning accuracy. Furthermore, it is recommended to perform further experimental tests at a range of different wind conditions. General gain tuning in these conditions will result in better performance. Next to that, research into different methods to calculate heading is suggested in order to allow stationary flight if the wind conditions allow for it. Some new manoeuvres such as a dynamic soaring cycle could also be used in order to increase the available energy extraction. Research into the presented lower limiting case can also show whether excess energy can be harvested and whether the feasible flying region can be extended. Finally, it is suggested to create an optimisation strategy for the positional requirements.

References

1. L. Miller, F. Gans, and A. Kleidon, "Estimating maximum global land surface wind power extractability and associated climatic consequences," *Earth System Dynamics*, vol. 2, 02 2011.
2. M. Jacobson and C. Archer, "Saturation wind power potential and its implications for wind energy," *Proceedings of the National Academy of Sciences of the United States of America*, vol. 109, pp. 15679–84, 09 2012.
3. Rayleigh, "The soaring of birds," *Nature*, pp. 534–535, 4 1883.
4. P. Richardson, "Upwind dynamic soaring of albatrosses and uavs," *Progress in Oceanography*, vol. 130, 11 2014.
5. P. Richardson, "How do albatrosses fly around the world without flapping their wings?," *Progress in Oceanography*, vol. 88, pp. 46–58, 03 2011.
6. G. Sachs, "In-flight measurement of upwind dynamic soaring in albatrosses," *Progress in Oceanography*, vol. 142, 01 2016.
7. E. Shepard, S. Lambertucci, D. Vallmitjana, and R. Wilson, "Energy beyond food: Foraging theory informs time spent in thermals by a large soaring bird," *PloS one*, vol. 6, p. e27375, 11 2011.
8. H. Weimerskirch, O. Chastel, and O. Tostain, "Frigate-birds ride high on thermals," *Nature*, 01 2003.
9. M. Allen, "Autonomous soaring for improved endurance of a small uninhabitated air vehicle," 01 2005.
10. G. Bousquet, M. Triantafyllou, and J.-J. Slotine, "Optimal dynamic soaring consists of successive shallow arcs," *Journal of The Royal Society Interface*, vol. 14, p. 20170496, 10 2017.
11. J. L. Grenestedt and J. R. Spletzer, "Towards perpetual flight of a gliding unmanned aerial vehicle in the jet stream," in *49th IEEE Conference on Decision and Control (CDC)*, pp. 6343–6349, 2010.
12. X.-Z. Gao, Z.-X. Hou, Z. Guo, R.-F. Fan, and X.-Q. Chen, "Analysis and design of guidance-strategy for dynamic soaring with uavs," *Control Engineering Practice*, vol. 32, p. 218–226, 11 2014.
13. C. Dunn, J. Valasek, and K. Kirkpatrick, "Unmanned air system search and localization guidance using reinforcement learning," *AIAA Infotech at Aerospace Conference and Exhibit 2012*, 01 2012.
14. T. Woodbury, C. Dunn, and J. Valasek, "Autonomous soaring using reinforcement learning for trajectory generation," 01 2014.
15. C. White, E. Lim, S. Watkins, A. Mohamed, and M. Thompson, "A feasibility study of micro air vehicles soaring tall buildings," *Journal of Wind Engineering and Industrial Aerodynamics*, vol. 103, pp. 41 – 49, 04 2012.
16. C. White, S. Watkins, E. Lim, and K. Massey, "The soaring potential of a micro air vehicle in an urban environment," *International Journal of Micro Air Vehicles*, vol. 4, pp. 1–14, 03 2012.
17. A. Mohamed, M. Abdulrahim, S. Watkins, and R. Clothier, "Development and flight testing of a turbulence mitigation system for micro air vehicles," *Journal of Field Robotics*, pp. 1–22, 08 2015.
18. A. Fisher, M. Marino, R. Clothier, S. Watkins, L. Peters, and J. Palmer, "Emulating avian orographic soaring with a small autonomous glider," *Bioinspiration & biomimetics*, vol. 11, p. 016002, 12 2015.

19. D. Lee, S. Longo, and E. Kerrigan, "Predictive control for soaring of unpowered autonomous uavs," vol. 4, pp. 194–199, 08 2012.
20. R. B. Patel, "Prohibited volume avoidance for aircraft," 2010.
21. P. S. Jackson and J. C. R. Hunt, "Turbulent wind flow over a low hill," *Quarterly Journal of the Royal Meteorological Society*, vol. 101, no. 430, pp. 929–955, 1975.